PHYSICAL REVIEW B **94**, 174431 (2016)

$3d$-electron Heisenberg pyrochlore $Mn_2Sb_2O_7$

Darren C. Peets,[1,2,*] Hasung Sim,[1,2] Maxim Avdeev,[3] and Je-Geun Park[1,2]
[1]*Center for Correlated Electron Systems, Institute for Basic Science (IBS), Seoul 08826, Korea*
[2]*Department of Physics and Astronomy, Seoul National University, Seoul 08826, Korea*
[3]*Australian Nuclear Science and Technology Organisation, Lucas Heights, New South Wales 2234, Australia*

(Received 18 August 2016; revised manuscript received 1 November 2016; published 21 November 2016; corrected 10 March 2017)

In frustrated magnetic systems, geometric constraints or the competition among interactions introduce extremely high degeneracy and prevent the system from readily selecting a low-temperature ground state. The most frustrated known spin arrangement is on the pyrochlore lattice, but nearly all magnetic pyrochlores have unquenched orbital angular momenta, constraining the spin directions through spin-orbit coupling. Pyrochlore $Mn_2Sb_2O_7$ is an extremely rare Heisenberg pyrochlore system with directionally unconstrained spins and low chemical disorder. We show that it undergoes a spin-glass transition at 5.5 K, which is suppressed by disorder arising from Mn vacancies, indicating this ground state to be a direct consequence of the spins' interactions. The striking similarities to $3d$ transition-metal pyrochlores with unquenched angular momenta suggests that the low spin-orbit coupling in the $3d$ block makes Heisenberg pyrochlores far more accessible than previously imagined.

DOI: 10.1103/PhysRevB.94.174431

I. INTRODUCTION

Strong frustration in which interactions compete impedes spin systems from selecting a unique global ground state at low temperatures, leading to a wide variety of physics in which fluctuations, quantum-mechanical effects, and fine details of the spin-spin interactions can be crucial [1]. Due to their extremely strong magnetic frustration, pyrochlore oxides and halides host a plethora of exotic phases, such as quantum spin liquids [2–4], or emergent magnetic monopoles [5–7] for classical spins. However, the spins in nearly every known magnetic pyrochlore are either Ising- or XY-like, constrained through spin-orbit coupling to point directly into or out of the tetrahedra on whose corners they reside or on a plane perpendicular and in no other direction. Pyrochlore lattices with directionally unconstrained Heisenberg spins are scarce and not as well studied. With far more degrees of freedom leading to far greater degeneracy but also a greater ability to adapt to interactions, Heisenberg pyrochlore systems may offer an immense potential for unveiling new physics [8].

Spin-orbit coupling, the interaction responsible for coupling spins to the crystal lattice thereby constraining their directions, strengthens as the atomic number increases. Heavy magnetic ions, such as the lanthanides most commonly encountered in the pyrochlore structure, are thus best considered in terms of spin-orbit-coupled j states linked to the lattice. A comparative lack of pyrochlores containing magnetic ions from earlier in the periodic table, particularly the $3d$ block, makes pure Heisenberg physics scarce in this lattice. The best-studied $3d$-electron pyrochlores, spinel oxides in which the B site forms a pyrochlore lattice, typically contain Cr^{3+} ($s = 3/2$) [9,10], whose orbital moments should not fully be quenched and may not behave as pure Heisenberg spins. To the authors' knowledge, only three known materials host pure Heisenberg spins in a pyrochlore lattice: FeF_3 [11,12], the pyrochlore variant of $Mn_2Sb_2O_7$ (pyr-$Mn_2Sb_2O_7$) [13–15], and the recently reported $NaSrMn_2F_7$ [16]. All have a high-spin $3d^5$-electron configuration with fully quenched orbital moments, and both FeF_3 and pyr-$Mn_2Sb_2O_7$ are challenging to prepare by conventional solid-state synthesis. Pyrochlore FeF_3 orders magnetically at 22 K [11,17], a more than tenfold suppression relative to its less-symmetric and less-frustrated rhombohedral polymorph [18], whereas the 2.7-K transition in $NaSrMn_2F_7$ also indicates very strong frustration. Curiously, pyr-$Mn_2Sb_2O_7$ has been reported to form a spin glass around 41 K [14,15], several times *higher* than the magnetic transition in its less-frustrated $P3_121$ polymorph [12,19,20]. With pyr-$Mn_2Sb_2O_7$ having a Curie-Weiss temperature just under 50 K, its putative 41-K transition would correspond to remarkably low frustration in the most-frustrated known three-dimensional magnetic lattice.

In a Heisenberg pyrochlore, the most likely magnetic ground state would be a counterpart of the all-in-all-out state found in Ising pyrochlore antiferromagnets, but the considerable degeneracy could make a variety of other states possible [8] or may prevent long-range order [21,22]. The lack of purely Heisenberg systems and the anomalously low frustration in pyr-$Mn_2Sb_2O_7$ have hampered the search for novel physics. We show that the spin-glass transition in pyr-$Mn_2Sb_2O_7$ is actually 5.5 K, corresponding to much higher frustration, and this transition is suppressed by Mn vacancies. The Mn^{2+} magnetic ion adopts a $3d^5$ high-spin electronic configuration with no orbital degree of freedom, leaving the spin directions fully unconstrained. The magnetic behavior is strikingly similar to that in several closely related $3d$ pyrochlores having unquenched orbital moments, indicating that the low spin-orbit coupling in the $3d$ transition metals may render a much broader family of materials as effective Heisenberg pyrochlore systems.

II. EXPERIMENTAL

When prepared by conventional solid-state synthesis, $Mn_2Sb_2O_7$ forms in a distorted chiral variant of the trigonal Weberite structure [19,23,24], but the desired pyrochlore

---

[*] Current address: State Key Laboratory of Surface Physics, Department of Physics and Advanced Materials Laboratory, Fudan University, Shanghai 200438, China; dpeets@fudan.edu.cn

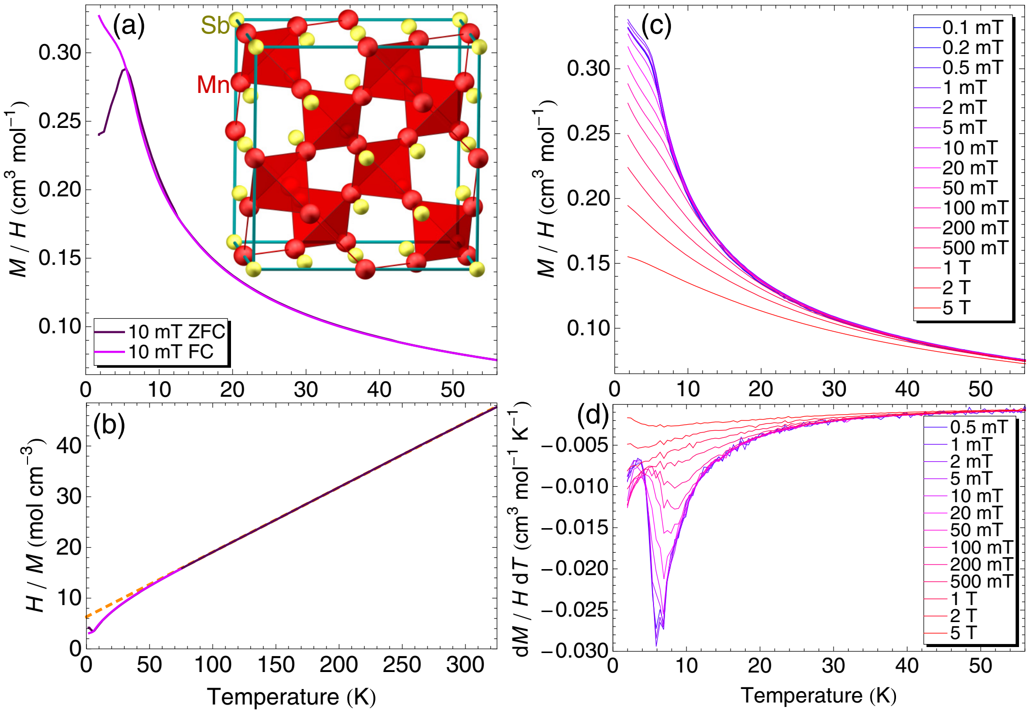

FIG. 1. Magnetization M/H of pyr-$Mn_2Sb_2O_7$. (a) Zero-field-cooled (ZFC) and field-cooled (FC) magnetizations in 10 mT show a transition at 5.5 K. (b) Inverse magnetization, showing a deviation from Curie-Weiss behavior (dashed line) below ~80 K. (c) Field dependence of the FC magnetization. (d) Temperature derivative of the data in (c). The crystal structure is depicted in the inset to (a), based on the structure refinement in the Supplementary Material [26], with Mn tetrahedra in red and the Sb sublattice in yellow.

polymorph [Fig. 1(a) inset] can be stabilized at lower temperatures [13–15]. We prepared powder samples of pyr-$Mn_2Sb_2O_7$ following Brisse *et al.* [13] with precursor "antimonic acid" prepared from $SbCl_5$ (Alfa Aesar, 99.997%) and deionized water as in Ref. [25]. The precursor was ground with $Mn(Ac)_2 \cdot 4H_2O$ (Sigma-Aldrich, 99.99%) then reacted for 12 h at a sequence of temperatures from 50 to 550 °C in Al_2O_3 crucibles in air. Powder diffraction and magnetic measurements were used to verify phase purity and Mn site occupancy.

X-ray powder-diffraction patterns were collected using a Bruker D8 Discover diffractometer with a Cu $K\alpha$ source, whereas a Rigaku Miniflex II was used to collect patterns on precursor antimonic acid and monitor reaction completeness. Magnetization measurements were performed in a Quantum Design magnetic property measurement system (MPMS-XL) magnetometer in a reciprocating sample measurement system measurement mode: An ~10-mg powder sample was gently compressed inside a gelatin capsule, which was closed with Kapton tape and inserted into a plastic straw. The sample holder contribution was below the noise level. ac susceptibility was measured in the same magnetometer using the dc sample transport at a zero applied field. Specific heat was measured on a thin plate of pressed powder by the relaxation time method in fields up to 9 T in a Quantum Design physical property measurement system. As an approximate phonon baseline, trigonal Weberite $Sr_2Sb_2O_7$ ceramic prepared by standard solid-state synthesis was used. Powder neutron diffraction was performed at the ECHIDNA diffractometer at the OPAL research reactor at ANSTO, Australia from 6.5° to 164° in steps of 0.05° with neutron wavelengths of 1.6220 Å (room temperature) and 2.4395 Å (low temperatures). Diffraction data were Rietveld refined in FULLPROF by the least-squares method [27]. Throughout this paper, molar quantities refer to formula units.

III. RESULTS AND DISCUSSION

The temperature-dependent dc magnetization of pyr-$Mn_2Sb_2O_7$, shown in Fig. 1, indicates a magnetic transition at $T_f = 5.5$ K, below which the zero-field-cooled and field-cooled magnetization data [Fig. 1(a)] diverge, implying that the spins order or freeze. This transition broadens and moves to higher temperatures in field [Fig. 1(c)], becoming indistinct above ~0.5 T. This is more clearly visible in the derivative [Fig. 1(d)], which also shows that there is no evidence for any other transition. In particular, the transition reported around 41 K [14,15] is absent. As shown in Fig. 1(b), above ~80 K the magnetization obeys the Curie-Weiss law with a Curie-Weiss temperature $T_{CW} = -49$ K indicating predominantly antiferromagnetic interactions. Deviations from Curie-Weiss behavior below ~80 K indicate the onset of short-range correlations more than an order of magnitude above T_f, whereas the approximately order-of-magnitude difference between T_{CW} and T_f indicates strong frustration. The paramagnetic moment of $5.59\mu_B$ is consistent with the spin-only expectation of $5.92\mu_B$ for high-spin $3d^5$, confirming the absence of an orbital contribution and demonstrating that pyr-$Mn_2Sb_2O_7$ is indeed a Heisenberg spin system.

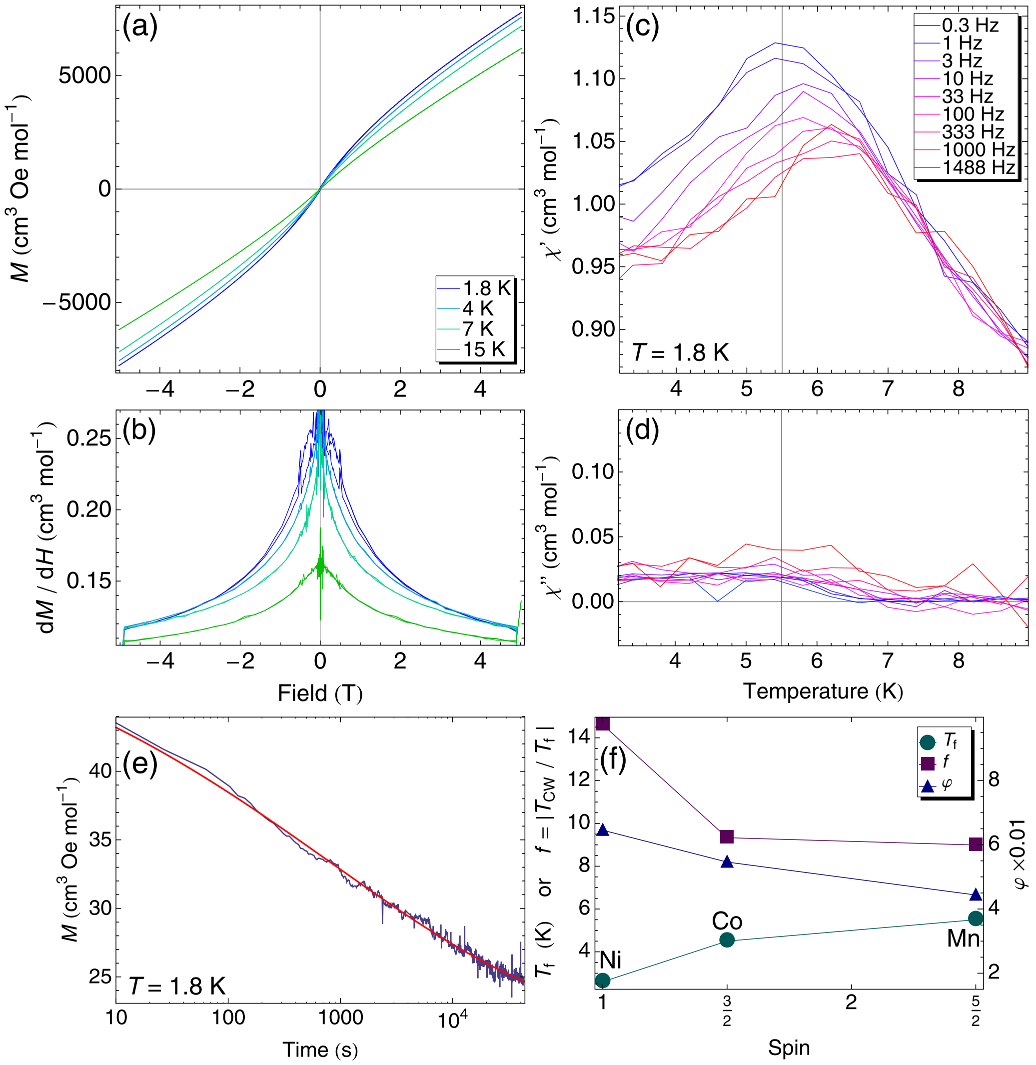

FIG. 2. Magnetic response of pyr-$Mn_2Sb_2O_7$. (a) $M(H)$ loops; slight hysteresis at 1.8 and 4 K is more evident in (b) the derivative dM/dH. The smooth field and temperature evolution show no evidence for an abrupt phase transition. Jumps in the derivative correspond to changes in sweep rate. (c) A broad peak in the real part of the zero-field ac susceptibility at $T_f = 5.5$ K, the same temperature identified in $M(T)$, shifts substantially as the drive frequency increases. (d) The loss χ'' is weakly positive below the transition. (e) Strong relaxation is visible at 1.8 K. The sample was cooled in a field of 0.1 T, then the field was removed, and the zero-field relaxation monitored. (f) Evolution of the intrinsic transitions and frustration in $M_2Sb_2O_7$ for M = Ni, Co, and Mn, based on Ref. [15].

The field dependence of the magnetization [Fig. 2(a)] is S shaped and exhibits hysteresis at low temperatures, which persists to at least 1.5 T with no clear onset field. The derivative [Fig. 2(b)] shows clearer evidence of the hysteresis and a lack of any sharp phase transition. Abrupt changes in the hysteresis loops where the field sweep rate was changed indicate strong relaxation effects on the time scale of minutes. To verify this, Fig. 2(e) shows the results of field training the sample by cooling to 1.8 K in a 0.1 T field, then monitoring the ensuing magnetization decay after reducing the field to zero. The magnetization is well described by a stretched exponential $M(t) = M_0 + M_R \exp[-(t/t_P)^{1-n}]$ [28,29] with a nonrelaxing offset $M_0 = 21.6(2)$ cm^3 Oe mol^{-1}, a substantial relaxing component $M_R = 31.7(14)$ cm^3 Oe mol^{-1}, time scale t_P of 835(112) s, and exponent n of 0.7843(97). An S-shaped hysteresis loop with rate- or time-dependent hysteresis is one key hallmark of a spin glass [27].

The zero-field ac susceptibility χ measured with an excitation amplitude of 1 Oe, shown in Figs. 2(c) and 2(d), also shows fingerprints of strong relaxation. A broad peak at low frequencies in the real component χ' agrees well with the magnetization transition, then shifts to significantly higher temperatures as the frequency increases. The imaginary component χ'' becomes weakly positive on cooling through the transition, indicating dissipation as the low-frequency measurement field aids the system in finding a ground state. By tracking the frequency dependence of the intrinsic low-temperature transition, the Mydosh parameter $\varphi = \Delta T_N / T_N \Delta \log f = 0.044$ can be extracted. This is comparable to 0.053 and 0.064 found for pyrochlore $Co_2Sb_2O_7$ and $Ni_2Sb_2O_7$, respectively [15], which undergo similar transitions into their low-temperature ground states. The three compounds' progression in transition temperatures, frustration factors $f \equiv |T_{CW}/T_f|$, and Mydosh parameters are plotted in Fig. 2(f), based on Ref. [15]. Given

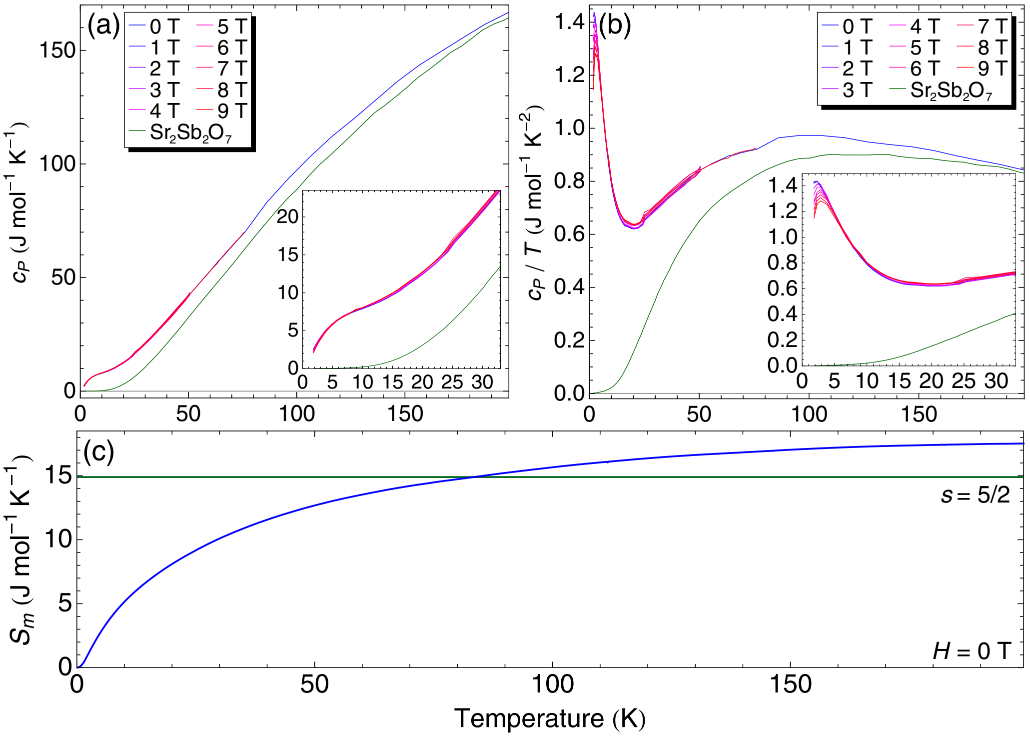

FIG. 3. Specific heat of pyr-$Mn_2Sb_2O_7$. (a) There is a hump in $c_P(T)$ at low temperatures and no feature around 41 K. Low-temperature data are highlighted in the inset, and data on Weberite $Sr_2Sb_2O_7$ serve as a baseline. (b) The broad peak in $c_P(T)/T$ is modified only slightly in field. Magnetic entropy is apparent to at least 40 K. (c) The approximate magnetic entropy calculated by subtracting the $Sr_2Sb_2O_7$ data. The entropy expected for $s = 5/2$ cannot all be found below ~20 K in the c_P/T peak.

that the Co and Ni analogs have unquenched orbital moments, the evolution is surprisingly mundane.

The specific heat in Fig. 3 shows a large and very broad hump of magnetic entropy at low temperatures, centered around 2.5 K, roughly half the temperature found *via* magnetization. It does not resemble a usual first- or second-order phase transition, and we have not attempted to extract any more precise estimates for the transition temperature. In applied magnetic fields the hump moves to higher temperatures as does the transition in the magnetization, but it also appears to narrow slightly. Such behavior is readily explained by the magnetic field relieving the frustration and is common in spin glasses. Specific heat data for $Sr_2Sb_2O_7$ [30], a nonmagnetic insulator forming in the related trigonal Weberite structure [31,32], are included for comparison. However, the phonons in pyr-$Mn_2Sb_2O_7$ clearly freeze-out at significantly lower temperatures, making any subtraction of the phonon background inexact. A very approximate measure of the magnetic entropy can be extracted by subtracting the $Sr_2Sb_2O_7$ data as a phonon background, but the only conclusion to be drawn here is that most of the entropy expected from $s = 5/2$ $3d^5$ is not released near the transition.

Low-temperature neutron-diffraction patterns collected through T_f are shown in Figs. 4(a) and 4(b). The transition introduces no new peaks nor significant changes to the intensities of existing peaks as further demonstrated by taking the difference across the transition. It is worth noting that there is no low-temperature structural transition that could reduce the frustration. Figure 4(c) highlights the presence of a diffuse magnetic component near the (111) nuclear Bragg peak at a d spacing of ~5.8 Å, which becomes indistinct above 20 K, in line with the magnetization and specific heat results. The temperature dependence is shown in Fig. 4(d), based on fitting each difference pattern to a Gaussian with a sloping background. pyr-$Mn_2Sb_2O_7$ now meets all the canonical criteria and has all the earmarks of a spin glass: the ZFC and FC magnetizations differ, strong relaxation is observed, the ac susceptibility is strongly frequency dependent, there is only a broad hump below the transition in the specific heat, and long-range order is absent.

Mn ions in pyr-$Mn_2Sb_2O_7$ populate an extremely high-symmetry lattice which should essentially be free from chemical disorder, so there should be nothing extrinsic to the spin system that could locally lock the spins and force a glass transition. Since pyr-$Mn_2Sb_2O_7$ most likely forms through substituting Mn atoms into the preexisting pyrochlore matrix of $Sb_2O_5 \cdot nH_2O$ [13], a manganese deficiency is possible, and manganese vacancies may be the dominant defect. X-ray diffraction indicated Mn deficiencies in incompletely reacted material and those prepared from Mn-poor mixtures, but the Mn site refined to full occupancy in all samples reported above. Mn-deficient samples show a significant suppression of T_f, often with no evidence for even the onset of a transition above 1.8 K but with much stronger field enhancement in the specific heat—an incompletely reacted example is shown in Fig. 5. This suppression by disorder strongly suggests that the magnetic freezing is intrinsic. As thermal fluctuations diminish on cooling, it presumably becomes more difficult to rotate any

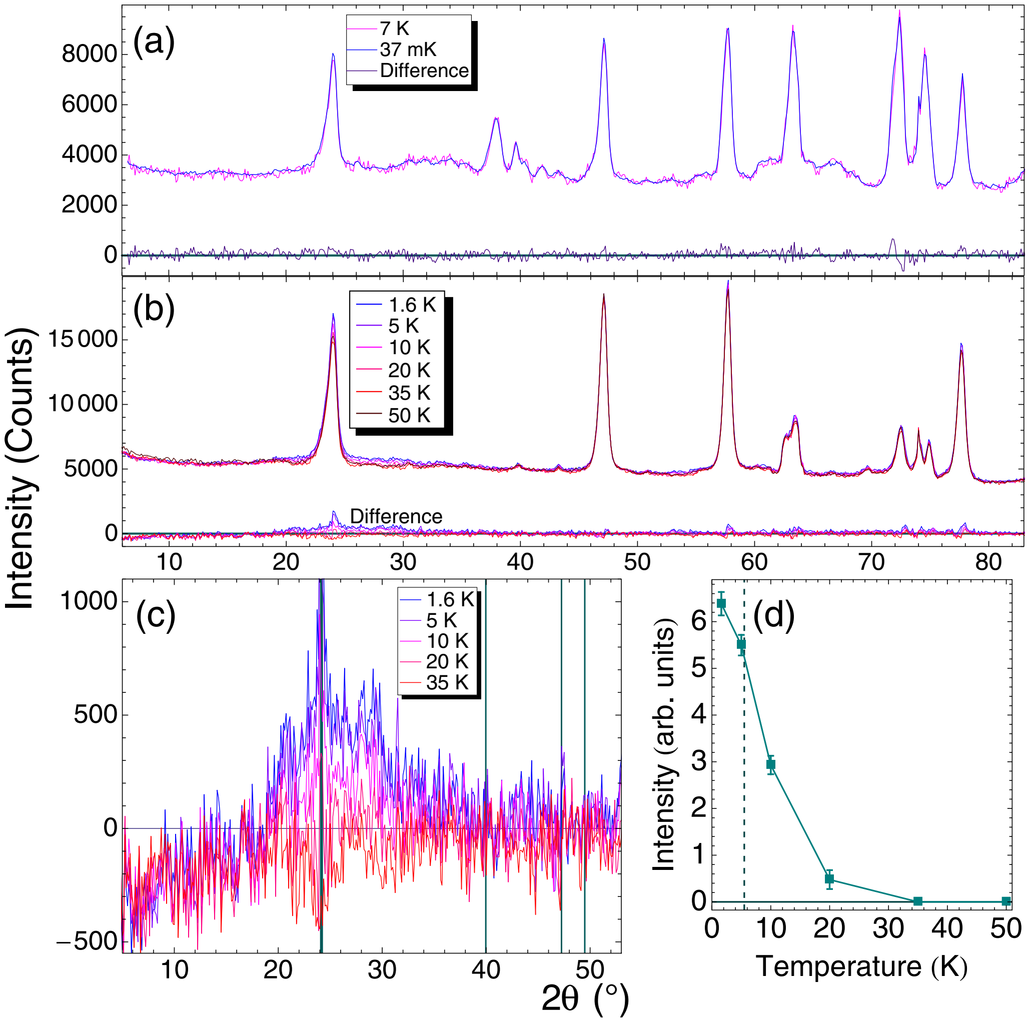

FIG. 4. Low-temperature neutron diffraction on pyr-$\mathrm{Mn_2Sb_2O_7}$. (a) and (b) Diffraction patterns at low temperatures, through T_f, demonstrate the absence of any new magnetic or structural peaks. Differences between (a) 7 K and 37 mK data and (b) from the 50 K data are shown. Several peaks originate from the sample holder—Cu in (a) and Al in (b). (c) Difference from data taken at 50 K, highlighting the diffuse contribution. Nuclear Bragg positions are marked. (d) Temperature dependence of the diffuse peak.

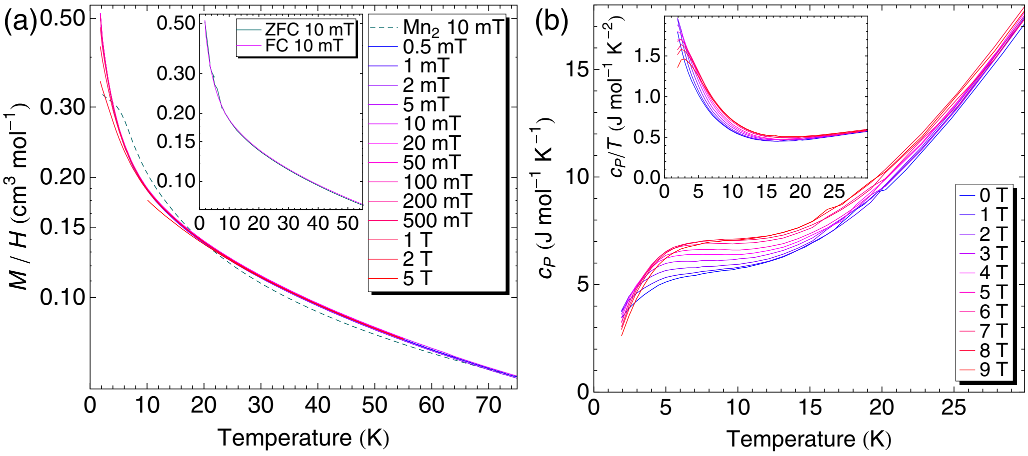

FIG. 5. Properties of Mn-deficient pyr-$\mathrm{Mn_2Sb_2O_7}$. (a) There is no transition in the field-cooled or zero-field-cooled (the inset) magnetization. (b) Magnetic fields shift the magnetic entropy to higher temperatures.

one spin because of the increasing number of spins coupled to it: effectively a diverging mass term. Intriguingly, this behavior is not observed in FeF_3, which enters an all-in-all-out magnetic ground state [18,33]. The latter has been explained through density functional theory [34], but similar calculations for pyr-$Mn_2Sb_2O_7$ have not been performed. In FeF_3 nearest-neighbor antiferromagnetic Heisenberg, biquadratic, and Dzyaloshinskii-Moriya interactions were all required to adequately model the spin system. In pyr-$Mn_2Sb_2O_7$, which has a smaller unit cell and rather different ligand coordination, these may be expected to have completely different strengths. In particular, the Mn tetrahedron in pyr-$Mn_2Sb_2O_7$ contains a central O2 atom, offering a much more direct exchange pathway. Modeling the interactions in this material and the resulting magnetic ground state will be an important avenue for future theoretical exploration.

One important question is why we observe a bulk ordering transition at 5.5 K while previous reports placed it around 41 K [14,15]. We attribute the previous results to trace quantities of unreacted Mn_3O_4, which has a ferrimagnetic transition around this temperature [35,36]. Samples which were Mn rich or incompletely reacted often exhibited a strong transition around 41 K in the magnetization even when phase pure by x-ray diffraction; however, there was no trace of the transition in the specific heat. Because the Mn_3O_4 ferrimagnetic moments are large and readily field trained, even trace quantities can dominate the low-field magnetization. This makes it crucial to completely eliminate this impurity if the intrinsic physics of pyr-$Mn_2Sb_2O_7$ are to be investigated. Previous measurements on pyr-$Mn_2Sb_2O_7$ display hints of intrinsic behavior at low temperatures in the inverse magnetization [14], but the data otherwise concentrate, understandably, on the obvious 41-K transition.

IV. CONCLUSION

To summarize, the 3*d*-electron Heisenberg pyrochlore pyr-$Mn_2Sb_2O_7$ undergoes a transition around 5.5 K into a spin-glass state with dominantly antiferromagnetic interactions. Short-range magnetic correlations survive to much higher temperatures, and strong frustration is evident. The manganese content can be tuned continuously from zero to full occupancy, offering a very interesting control knob for future disorder studies. Measurements at lower temperatures will be required to establish whether the specific heat resembles that in kagome order-by-disorder systems [37–39]. The physical properties of pyr-$Mn_2Sb_2O_7$ bear a striking similarity to those of the magnetic pyrochlores $Ni_2Sb_2O_7$ and $Co_2Sb_2O_7$ [15] and more recently $NaSrCo_2F_7$, $NaCaNi_2F_7$, $NaCaFe_2F_7$, and $NaSrFe_2F_7$ [16,40,41], which should all have unquenched orbital moments. This suggests that spin-orbit coupling may be so weak in 3*d* transition-metal pyrochlores as to be effectively irrelevant to the frustrated spins, greatly broadening the suite of materials available for investigating effective Heisenberg physics on the most-frustrated known three-dimensional lattice. The very recently reported $NaSrMn_2F_7$ [16] with quenched orbital moments but *A*-site cation disorder also behaves in a similar manner.

ACKNOWLEDGMENTS

This work was supported by the Institute for Basic Science (IBS) in Korea (Grant No. IBS-R009-G1). The authors thank M. Gingras for stimulating discussions. We acknowledge support of the Bragg Institute, Australian Nuclear Science and Technology Organisation in providing the neutron research facilities used in this paper.

---

[1] *Introduction to Frustrated Magnetism*, edited by C. Lacroix, P. Mendels, and F. Mila, Springer Series in Solid-State Sciences (Springer, Berlin, 2011), Vol. 164.
[2] J. S. Gardner, M. J. P. Gingras, and J. E. Greedan, Rev. Mod. Phys. **82**, 53 (2010).
[3] L. Balents, Nature (London) **464**, 199 (2010).
[4] K. A. Ross, L. Savary, B. D. Gaulin, and L. Balents, Phys. Rev. X **1**, 021002 (2011).
[5] C. Castelnovo, R. Moessner, and S. L. Sondhi, Nature (London) **451**, 42 (2008).
[6] D. J. P. Morris, D. A. Tennant, S. A. Grigera, B. Klemke, C. Castelnovo, R. Moessner, C. Czternasty, M. Meissner, K. C. Rule, J.-U. Hoffmann, K. Kiefer, S. Gerischer, D. Slobinsky, and R. S. Perry, Science **326**, 411 (2009).
[7] T. Fennell, P. P. Deen, A. R. Wildes, K. Schmalzl, D. Prabhakaran, A. T. Boothroyd, R. J. Aldus, D. F. McMorrow, and S. T. Bramwell, Science **326**, 415 (2009).
[8] Y. Wan and M. J. P. Gingras, Phys. Rev. B **94**, 174417 (2016).
[9] S.-H. Lee, C. Broholm, W. Ratcliff, G. Gasparovic, Q. Huang, T. H. Kim, and S.-W. Cheong, Nature (London) **418**, 856 (2002).
[10] K. Tomiyasu, H. Suzuki, M. Toki, S. Itoh, M. Matsuura, N. Aso, and K. Yamada, Phys. Rev. Lett. **101**, 177401 (2008).
[11] R. De Pape and G. Ferey, Mater. Res. Bull. **21**, 971 (1986).
[12] J. N. Reimers, J. E. Greedan, C. V. Stager, M. Bjorgvinnsen, and M. A. Subramanian, Phys. Rev. B **43**, 5692 (1991).
[13] F. Brisse, D. J. Stewart, V. Seidl, and O. Knop, Can. J. Chem. **50**, 3648 (1972).
[14] H. D. Zhou, C. R. Weibe, A. Harter, N. S. Dalal, and J. S. Gardner, J. Phys.: Condens. Matter **20**, 325201 (2008).
[15] H. D. Zhou, C. R. Wiebe, J. A. Janik, B. Vogt, A. Harter, N. S. Dalal, and J. S. Gardner, J. Solid State Chem. **183**, 890 (2010).
[16] M. B. Sanders, J. W. Krizan, K. W. Plumb, T. M. McQueen, and R. J. Cava, arXiv:1608.02907.
[17] Y. Calage, M. Zemirli, J. Greneche, F. Varret, R. De Pape, and G. Ferey, J. Solid State Chem. **69**, 197 (1987).
[18] G. Ferey, R. DePape, M. Leblanc, and J. Pannetier, Rev. Chim. Miner. **23**, 474 (1986).
[19] D. C. Peets, H. Sim, M. Avdeev, and J.-G. Park, arXiv:1611.02811.
[20] The $P3_121$ polymorph of $Mn_2Sb_2O_7$ consists of alternating kagome and triangular Mn layers as in the pyrochlore structure but shifted to produce a very different chiral structure. A detailed study on the $P3_121$ polymorph is presented separately [19].

[21] R. Moessner and J. T. Chalker, Phys. Rev. Lett. **80**, 2929 (1998).

[22] R. Moessner and J. T. Chalker, Phys. Rev. B **58**, 12049 (1998).

[23] H. G. Scott, J. Solid State Chem. **66**, 171 (1987).

[24] L. Chelazzi, T. B. Ballaran, G. O. Lepore, L. Bindi, and P. Bonazzi, Solid State Sci. **21**, 85 (2013).

[25] D. J. Stewart and O. Knop, Can. J. Chem. **48**, 1323 (1970).

[26] See Supplemental Material at http://link.aps.org/supplemental/10.1103/PhysRevB.94.174431 for a crystal structure refinement of pyr-$Mn_2Sb_2O_7$.

[27] J. Rodríguez-Carvajal, Physica B **192**, 55 (1993).

[28] J. A. Mydosh, Hyperfine Interact. **31**, 347 (1986).

[29] K. Binder and A. P. Young, Rev. Mod. Phys. **58**, 801 (1986).

[30] O. Knop, G. Demazeau, and P. Hagenmuller, Can. J. Chem. **58**, 2221 (1980).

[31] W. Verscharen and D. Babel, J. Solid State Chem. **24**, 405 (1978).

[32] L. Cai and J. C. Nino, Acta Crystallogr., Sect. B: Struct. Sci. **65**, 269 (2009).

[33] J. N. Reimers, J. E. Greedan, and M. Björgvinsson, Phys. Rev. B **45**, 7295 (1992).

[34] A. Sadeghi, M. Alaei, F. Shahbazi, and M. J. P. Gingras, Phys. Rev. B **91**, 140407 (2015).

[35] K. Dwight and N. Menyuk, Phys. Rev. **119**, 1470 (1960).

[36] G. B. Jensen and O. V. Nielsen, J. Phys. C **7**, 409 (1974).

[37] A. P. Ramirez, G. P. Espinosa, and A. S. Cooper, Phys. Rev. Lett. **64**, 2070 (1990).

[38] J. T. Chalker, P. C. W. Holdsworth, and E. F. Shender, Phys. Rev. Lett. **68**, 855 (1992).

[39] I. Ritchey, P. Chandra, and P. Coleman, Phys. Rev. B **47**, 15342 (1993).

[40] J. W. Krizan and R. J. Cava, Phys. Rev. B **92**, 014406 (2015).

[41] J. W. Krizan and R. J. Cava, J. Phys.: Condens. Matter **27**, 296002 (2015).